

CHARACTERIZATION AND PHASE TRANSFORMATION STUDY OF TlSbSe₂ CRYSTALS*

K. Chrissafis^{1**}, M. Ozer², E. Vinga¹, E. Polychroniadis¹, X. Chatzistavrou¹ and K. M. Paraskevopoulos¹

¹Solid State Physics Section, Physics Department, Aristotle University of Thessaloniki, 54124 Thessaloniki, Greece

²Department of Physics, Istanbul Kultur University, Istanbul, Turkey

TlSbSe₂ monocrystals were grown using the modified Bridgman–Stockbarger method and were characterized by transmission electron microscopy (TEM) and X-ray diffraction (XRD). Reflectivity spectra have been registered in the range 50 to 4000 cm⁻¹ for E parallel to *a* and E parallel to *b* polarizations, on the cleavage plane. A remarkable anisotropy at two directions was verified. With regard to previous observations, additional peaks were discriminated and the fundamental phonon parameters were determined using classical dispersion relations. The material presents a complex phase transformation – with two thermal effects – that was examined using differential scanning calorimetry (DSC). Non-isothermal measurements, at different heating and cooling rates (β), were used to study the thermal phenomena. The main effect is attributed to a structural displacement and the second one to a cation exchange procedure. The phase transformation temperature depends strongly on the cooling rate and the peaks are shifted by 30 K with the increase of this rate, on the contrary to the increase of the heating rate that has a smaller effect. Phenomena related with the influence of the previous, repeated heating and cooling cycles on the transformation are also examined and analytically discussed.

Keywords: non-isothermal calculations DSC, phase transformation, polarized reflectivity spectra, TlSbSe₂

Introduction

TlSbSe₂ is characterized by its cleavage, by the strong anisotropy of its natural properties and its phase transformations. Also, it presents interesting semiconducting properties [1–7]. Its high light sensitivity and its low surface state density had resulted in its vast use in the production of MTIS leds (metal thin insulator-semiconductor) and layered semiconductor crystals.

TlSbSe₂ presents two-phase transformations. The phase of high temperature (HT) is orthorhombic with the atoms of Tl and Sb being statistically allocated to the positions of the cations. On the contrary, the allocation of the cations at the low temperature phase is strongly ordered. At room temperature, (RT) Wacker *et al.* [8, 9] found out that the crystals belong to the monoclinic system, with a space group such as P2₁ (C₂²) and lattice parameters $a=9.137 \text{ \AA}$, $b=4.097 \text{ \AA}$, $c=12.765 \text{ \AA}$, $\beta=111.75^\circ$. Between the high temperature phase and the room temperature one, there is an additional phase, which is partially ordered (PO) [10]. Kiosse *et al.* [11] showed that depending on the mode of the thermal process of the sample, it is possible to exist in two different structures: a monoclinic one with a possible space group C2/m or C2 and an orthorhombic one with Cmmm or C222.

The aim of this work is to characterize the grown material, TlSbSe₂, through TEM microscopy and FTIR spectroscopy in two directions to study its phase transformation.

Experimental

The growth of the monocrystals was realized with the Bridgman method. The original materials – of 99.999% purity for the Tl and Se and of greater than 99% purity for the Sb – were placed in stoichiometric ratio in a quartz ampoule, which was sealed under a vacuum better than 10⁻⁵ Torr. The ampoule was placed in a vertical furnace and it was held at a temperature higher than the melting points of the ingredients and of the final product, for 48 h. After that, the ampoule started to go down mechanically so as to slowly cool down to room temperature. The speed during the cooling process was accurately measured in the area of the melting point of TlSbSe₂ at 1.5 K h⁻¹. The grown crystals were characterized by XRD and TEM. For the study with the X-rays, a powder diffractometer with CuK α radiation was used. The TEM study was conducted with a JEM100C microscope at an operation voltage of 100 kV.

* Presented at MEDICTA Conference 2005, Thessaloniki, peer reviewed paper.

** Author for correspondence: hrisafis@physics.auth.gr

The thermal measurements were carried out using Setaram DSC141 unit. Temperature and energy calibrations of the instrument were performed at different heating rates, using the melting temperatures and melting enthalpies of high-purity zinc, tin and indium supplied with the instrument. The samples used that were in powder form and weighed about 50 mg, were crimped in aluminum crucibles and an empty aluminum crucible was used as reference. A constant nitrogen flow was maintained to provide a constant thermal blanket within the DSC cell, thus eliminating thermal gradients and ensuring the validity of the applied calibration standard from sample to sample.

The reflectivity spectra of the TlSbSe_2 crystals were taken for each sample, from a freshly cleaved surface, at two polarizations, in the spectral region $30\text{--}5000\text{ cm}^{-1}$ ($3.7\text{ meV--}0.62\text{ eV}$). The FTIR spectra were collected using a Bruker IFS113V spectrophotometer working under vacuum. In MIR region of $400\text{--}5000\text{ cm}^{-1}$, all spectra were received using a MIR polarizer, consisting of $0.12\text{ }\mu\text{m}$ wide strips of aluminium on a KRS substrate, while in FIR region of $30\text{--}400\text{ cm}^{-1}$, the used FIR polarizer consisted of aluminium grids deposited on a polyethylene substrate. Polarizer was mounted on a special holder with an appropriate stepping motor.

Results and discussion

The slow growth of the crystalline material and also, the prolonged stay of the structural material at a high temperature, created the necessary conditions for the structural arrangement of the material in its more energetically stable form. In Fig. 1 a typical diffractogram of the grown crystals is presented. The lattice parameters were determined using the Rietveld method, and were found to be $a=9.13\text{ \AA}$, $b=4.10\text{ \AA}$, $c=12.75\text{ \AA}$ and $\beta=111.63^\circ$. These values are in very good coincidence with those from the literature [12]. From the images of electron diffraction (Fig. 2), the characteristic hkl indices of the diffraction spots and the assessment of the zone axis of the diffraction patterns are identified with accuracy.

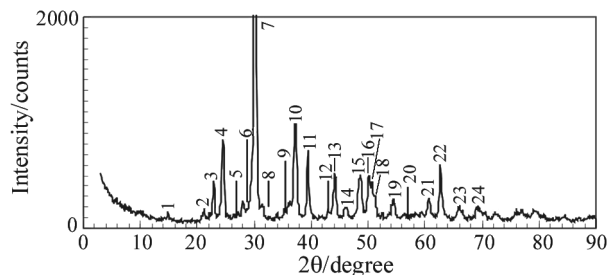


Fig. 1 X-ray diffraction pattern

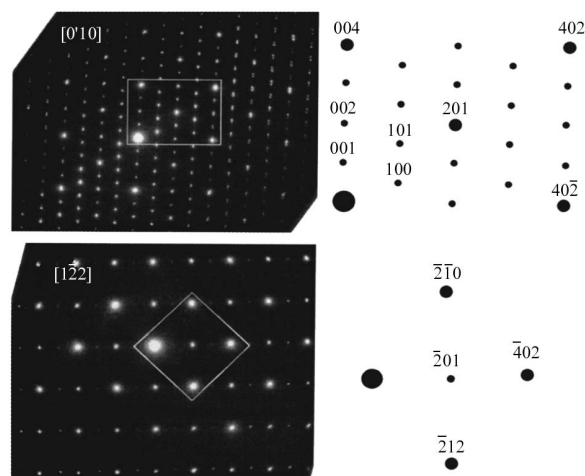


Fig. 2 Electron diffraction pattern

Both, the X-ray analysis data of samples taken from different parts of the grown crystal and the observations at microscopic level with the use of the TEM, suggest that the material is homogeneous and belongs to the monoclinic system, which coincides with that of Wacker *et al.* [12]. The vertical direction at the cleavage plane was found to be the $[010]$ one of the monoclinic symmetry.

In Fig. 3 are presented the reflectivity spectra of the crystal at two directions, in FIR region. The characteristic reflectance bands appear in the frequency range of $60\text{--}200\text{ cm}^{-1}$, while at higher wavenumbers there is not any characteristic peak. The spectra at the two different directions ($E//b$ and $E//a$), confirm the existence of a major anisotropy. From the comparison of the spectra of Fig. 3 with those measured by Syrbu *et al.* [13], it is clear that there are differences in their characteristics, but mainly, we observe the appearance of new peaks. The new peaks are attributed to discrete phonons. The number of phonons in the spectrum of the

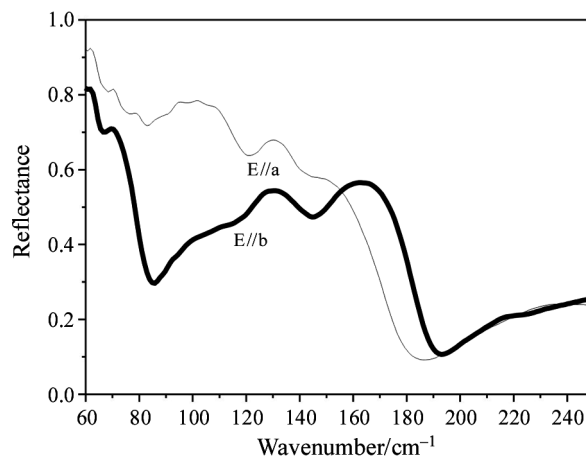


Fig. 3 Reflectivity spectra of TlSbSe_2 crystal for $E//b$ and $E//a$ polarizations

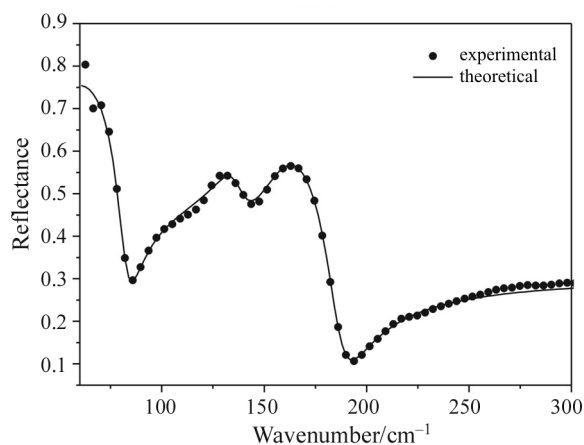


Fig. 4 Reflectivity spectrum of TlSbSe₂ crystal for E//b polarization, fitted by a theoretical curve

crystal – which is crystallized at the monoclinic system – is not clearly defined. The attribution of the reflectance spectrum peaks can be done by the theoretical analysis of the band structure of TlSbSe₂ (Fig. 4).

The reflectivity spectra were fitted by a complex dielectric function in the form of a sum of four classical Lorentz oscillator terms, according to Eq. (1):

$$\varepsilon(\omega) = (n - ik)^2 = \varepsilon_{\infty} + \sum_{j=1}^4 \frac{\Delta\varepsilon_j \omega_{TOj}^2}{\omega^2 - \omega_{TOj}^2 - i\omega\gamma_{TOj}} \quad (1)$$

where n and k are the refractive and absorption indices respectively, ε_{∞} is the high-frequency dielectric constant, $\Delta\varepsilon$ the oscillator strength, and γ_{TO} is the phonon damping constant [14]. By varying the parameters of each oscillator in order to obtain the best fit of the theory to the reflectivity data, we obtained accurate values of the TO-modes' parameters ω_{TOj} , $\Delta\varepsilon_j$ and γ_{TOj} . In Table 1 the typical parameters from the analysis are presented.

The main difference between the reflectivity spectra of TlSbSe₂ crystal for E//b and E//a polarizations is observed in the frequency region of 150–180 cm⁻¹. Particularly, the strong oscillator in the reflectivity spectrum for the E//b polarization is presented at ~170 cm⁻¹, while the respective strong oscillator for the E//a polarization is slightly shifted towards lower wavenumbers and appears at ~160 cm⁻¹. In both cases, this mode – peak – is associated with the vibration of the Sb–Se atoms in the molecule and further-

Table 1 Oscillator parameters from fitting of reflectivity measurements

Phonon	$\omega_{TO}/\text{cm}^{-1}$	$\gamma_{\tau}/\text{cm}^{-1}$	$\Delta\varepsilon$
1 st	159	24.9	4.6
2 nd	134	16.0	2.6
3 rd	59	20.0	51.4
4 th	49	1.2	$0.88 \cdot 10^{-2}$

more its strength is determined by the oscillation within the layer of Sb–Se. Consequently, this observed shift of the position of the strong oscillator in the reflectivity spectra for E//b and E//a polarizations, is attributed to the difference between the interatomic distances of Sb–Se in the direction parallel to a , and parallel to b . It is known from the X-ray results, that the interatomic distance of Sb–Se is 9.13 Å, when this bond is parallel to a , and 4.10 Å when this bond is parallel to b . It is clearly seen that in the second case the length of the bond of Sb–Se is shorter and therefore we observed the position of the corresponding phonon at higher wavenumbers [13].

A full temperature cycle of the material (heating-cooling), taken at a rate $\beta = 5 \text{ K min}^{-1}$, is shown in Fig. 5. At both curves a composite phase transformation with two thermal events (double peak) is observed, with a significant hysteresis at the transformation temperature T_p (653–608 K). The main peak of these two thermal events may be attributed to a structural displacement, while the smaller one is the result of the cations exchange procedure. The cooling curve describes the material transformation from the high temperature phase (HT) to the partially ordered phase (partially ordered, PO). When studying polycrystalline and monocrystalline TlSbSe₂ with DTA, Kiosse *et al.* [8] recorded one more transformation at 553 K which we did not observe at all. The main reason for this is due to the fact that, different methods of material production might lead to a metastable orthorhombic structure of the material at room temperature and, as a consequence, to a different thermal behavior, as referred in the literature.

The temperature at which the phase transformation takes place depends strongly on the cooling rate as it is observed in Fig. 6, where the exothermic DSC cooling curves are given at various rates β (1, 2.5, 5 and 10 K min⁻¹). It is observed that with the increase of the cooling rate, the peaks are shifted towards

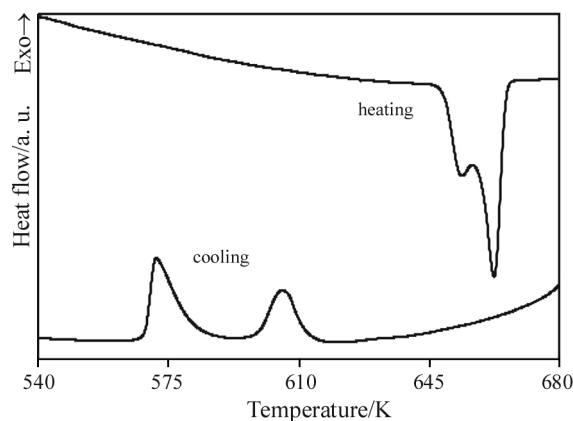


Fig. 5 Cycle of heating and cooling with rate 5 K min⁻¹

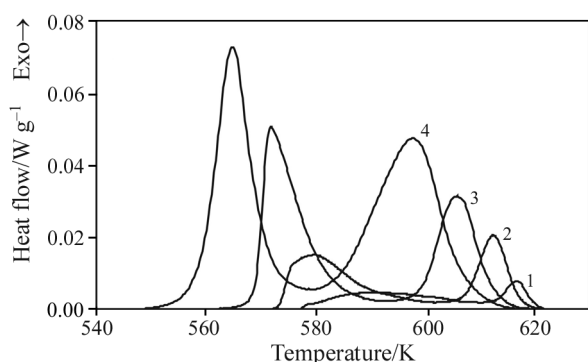


Fig. 6 DSC curves for different cooling rates β . 1: $\beta=1$, 2: $\beta=2.5$, 3: $\beta=5$, 4: $\beta=10$ K min^{-1}

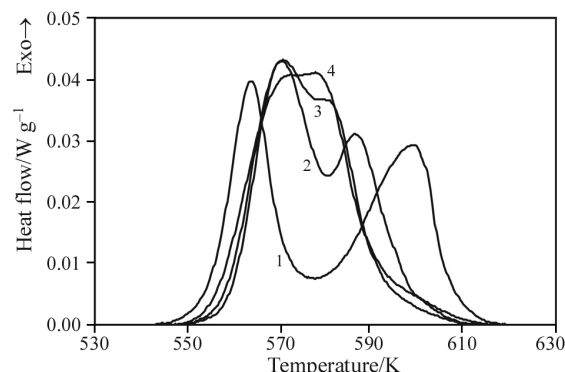


Fig. 8 DSC cooling curves after different numbers of repeated cycles: 1: 1st cycle, 2: 5th cycle, 3: 10th cycle, 4: 13th cycle

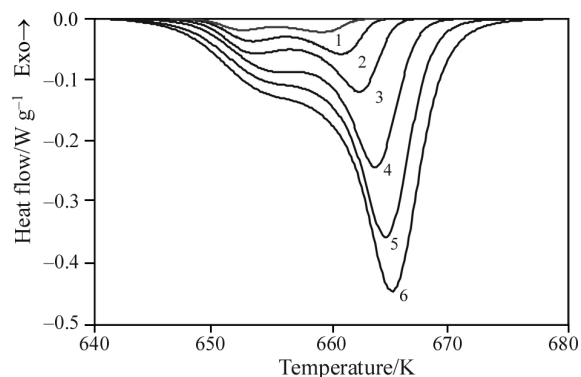


Fig. 7 DSC curves for different heating rates β . 1: $\beta=1$, 2: $\beta=2.5$, 3: $\beta=5$, 4: $\beta=10$, 5: $\beta=15$, 6: $\beta=20$ K min^{-1}

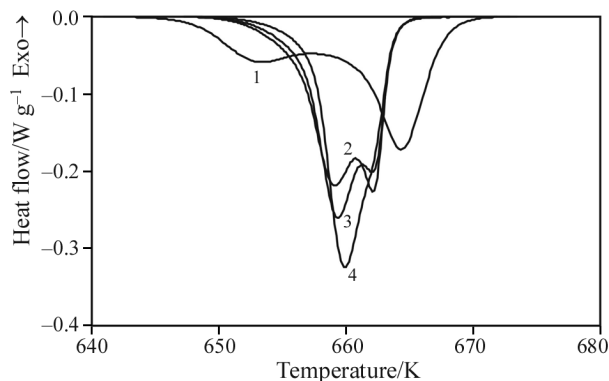


Fig. 9 DSC heating curves after different numbers of repeated cycles: 1: 1st cycle, 2: 3rd cycle, 3: 5th cycle, 4: 13th cycle

lower temperatures (about 30 K). At the heating process (Fig. 7), an increase of its rate causes a smaller than in the cooling process shift (7 K) towards higher temperatures. Therefore, this transformation is concluded to be thermally stimulated and this fact was not observed by Salk *et al.* [4]. Afterwards, the effect of the successive thermal processes (i.e. heating up to 683 K and cooling down to 443 K) on the phase transformation, was studied. Figures 8 and 9 show the DSC curves of the material for the cooling and heating procedures respectively, at a rate of 7.5 K min^{-1} . The results are recorded for several cycles of heating and cooling of the material. In the case of cooling (Fig. 8) it is observed that as the number of the repeated cycles is increased, the peaks move to opposite direction approaching to each other. So, while they are far away from each other at first (1st cycle), at the 13th cycle they have already almost been overlapped.

The same behaviour is observed also during the heating procedure (Fig. 9), with the peaks having been completely overlapped after the 13th cycle. Therefore, it is observed that the previous, repeated heating and cooling cycles of the material influence the transformation [15, 16].

From the thermal study of the material it is concluded that the shape, the height, as well as the posi-

tion of the peaks of the endothermic and exothermic phenomena depend on the heating-cooling rate and on the previous, repeated heating and cooling cycles of the material. From the elaboration of the DSC results it is found that the mean value of the transformation enthalpy is 5.7 ± 0.2 kJ mol^{-1} during heating and 4.2 ± 0.2 kJ mol^{-1} at cooling.

Conclusions

TlSbSe₂ crystals that were grown by the Bridgman method, were identified by XRD and TEM and were found homogeneous and to belong to the monoclinic system. The polarized reflectivity spectra for two directions show the existence of a remarkable anisotropy. Regarding previous observations, additional peaks were observed as well as altered characteristics, which are attributed to distinguished phonons the number of which is not known with accuracy. The main alteration observed in the polarized reflectivity spectra is attributed to the difference in the length of the Sb-Se bond, in the two directions. The DSC curves for the heating and cooling, present a composite phase transformation with two thermal events. The different heating and cooling rates cause the peak

shifts towards higher or lower temperatures respectively, both being thermally stimulated. The succession of the heating–cooling cycles results in the gradual shift of the two peaks to an opposite direction that leads to an almost complete overlap of the two curves after 13 cycles. This means that the previous repeated heating and cooling cycles of the material influence significantly the transformation.

References

- 1 D. V. Gitsu, I. N. Grincheshen, V. F. Krasovskii and N. S. Popovich, *Sov. Phys. Semicond.*, 22 (1988) 94.
- 2 I. N. Grincheshen, N. S. Popovich and A. A. Shtanov, *Phys. Stat. Sol., A*, 85 (1984) K85.
- 3 D. V. Gitsu, I. N. Grincheshen and N. S. Popovich, *Phys. Stat. Sol., A*, 72 (1982) K113.
- 4 M. Salk, K. Wacker, J. Fischer and V. Kramer, *Thermochim. Acta*, 160 (1990) 87.
- 5 J. Banyas, J. Grigas, V. Valiukenas and K. Wacker, *Solid State Commun.*, 82 (1992) 633.
- 6 J. Ren, M. H. Whango, H. Bengel, H. J. Cantow and S. N. Magonov, *Chem. Mater.*, 5 (1993) 1018.
- 7 K. Ulutas, N. Kalkan, S. Yildirim and D. Deger, *Cryst. Res. Technol.*, 40 (2005) 898.
- 8 K. Wacker and P. Buck, *Mater. Res. Bull.*, 15 (1980) 1105.
- 9 K. Wacker, M. Salk, G. Decker-Schultheiss and E. Keller, *Z. Anorg. Allg. Chem.*, 606 (1991) 51.
- 10 F. Gervais, *Infrared and Millimeter Waves*, 8, Academic Press, New York 1983, p. 279.
- 11 G. A. Kiosse, S. V. Ursakii, I. N. Grincheshen and K. R. Zbigli, *Sov. Phys. Crystallogr.*, 35 (1990) 431.
- 12 JCPDS-ICDD, X-ray Powder Data File (American Society for Testing Materials) Card No 76-2039.
- 13 N. N. Syrbu, V. T. Krasovsky and I. N. Grincheshen, *Cryst. Res. Technol.*, 28 (1993) 371.
- 14 R. Ferrini, G. Guizzetti, M. Patrini, A. Bosacchi, S. Franchi and R. Magnanini, *Solid State Commun.*, 104 (1997) 747.
- 15 T. Ozawa, *J. Therm. Anal. Cal.*, 72 (2003) 337.
- 16 Y. Wang and J. F. Mano, *J. Therm. Anal. Cal.*, 80 (2005) 171.

Received: August 1, 2005

Accepted: December 22, 2005

OnlineFirst: June 27, 2006

DOI: 10.1007/s10973-005-7213-7